Langmuir

ARTICLE

pubs.acs.org/Langmuir

# Formation of Bimetallic Au−Pd and Au−Pt Nanoparticles under Hydrothermal Conditions and Microwave Irradiation

Oleg V. Belousov,*[,†] Nataliya V. Belousova,[‡] Anastasia V. Sirotina,[‡] Leonid A. Solovyov,[†] Anatoly M. Zhyzhaev,[†] Sergey M. Zharkov,[‡,§] and Yuri L. Mikhlin[†]

[†]Institute of Chemistry and Chemical Technology of the Russian Academy of Sciences, Krasnoyarsk 660049, Russia

[‡]Siberian Federal University, Krasnoyarsk 660041, Russia

[§]L. V. Kirensky Institute of Physics of the Russian Academy of Sciences, Krasnoyarsk 660036, Russia



**ABSTRACT:** The reduction of chlorocomplexes of gold(III) from muriatic solutions by nanocrystal powders of palladium and platinum at 110 and 130 °C under hydrothermal conditions and the action of microwave irradiation has been investigated. The structure and composition of the solid phase have been characterized by transmission electron microscopy, X-ray diffraction, X-ray photoelectron spectroscopy, and chemical methods. Bimetallic particles with a core−shell structure have been revealed. The obtained particles are established to have a core of the metal reductant covered with a substitutional solid (Au, Pd) solution in case of palladium, and isolated by a gold layer in the case of platinum. The main reason for such a difference is the ratio between the rates of aggregation and reduction. It has been shown by the example of the Au−Pd system that the use of microwave irradiation allows us not only to accelerate the synthesis of particles but also to obtain more homogeneous materials in comparison with conventional heating.

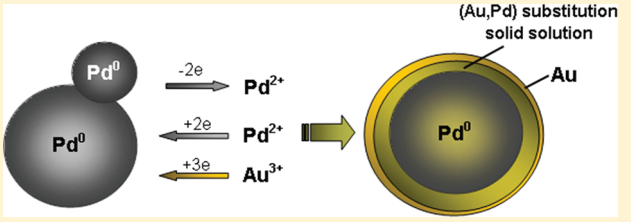


## INTRODUCTION

In recent years, various nanomaterials and particularly noble metal nanoparticles have been of great scientific and technological interest because of their unique optical, chemical and catalytic properties, which differ from those of bulk materials.[1] They have many potential applications in optoelectronics, semiconductors, catalysis, drug delivery, and other areas.[2] In recent decades, scientists have paid a great deal of attention to nanoparticles consisting of two sorts of metals (i.e., bimetallic particles). Some of their major properties and catalytic properties in particular have been proven to be superior to those of monometallic nanoparticles.[3]

Au−Pd and Au−Pt nanoparticles are the most significant in practice. Au−Pd- and Au−Pt-based catalysts are perfectly suitable for solving the problems of air purification, decreasing the temperature of the combustion of auto gas, and hydrogen purification for fuel elements.[4]

At present, there are many papers concerning the synthesis and structures of bimetallic particles. Most researches agree that the structure of the obtained materials (a mechanical mixture, a solid solution, or a "core−shell" structure) is defined by the synthesis conditions and physicochemical features of binary systems.

The main approaches to the methods of chemical synthesis of bimetallic nanoparticles can be reduced to the successive or simultaneous reduction of noble metals from solutions of their complex compounds. Thus, there are a great number of reduction methods in use for different reducing agents (sodium borohydride,[5,6] hydrazine,[7] phosphotungstic acid,[8] trisodium citrate, and ascorbic acid[9]) both in aqueous media and in organic solvents (methanol, ethanol, and *N*,*N*-dimethylformamide). Among the latter ones, polyols are growing in popularity. They act simultaneously as a solvent and a reducing agent.[2,10,11]

Some authors synthesized bimetallic particles with the core−shell structure. In most cases, the obtained bimetallic systems consisted of a gold core surrounded by a shell of another noble metal.[2,8,10] Sometimes the materials had multiple structures, for example, triple-layered ones.[12]

Cementation is one of the most effective methods of synthesis of bimetallic nanoparticles. The reactions of the contact reduction of noble metals from solution by nanocrystal powders are relevant to making materials with the given properties for such applications as coatings, obtaining polymetallic powders with different dispersities and various chemical and phase compositions.

Carrying out the processes under hydrothermal conditions with the use of autoclave technologies is a high-performance way to intensify the aforementioned reactions. It is especially important for experiments with platinum group metals. The processes with their participation are allowed thermodynamically but are often inhibited kinetically. The use of autoclave technologies allows the elimination of such kinetic limitations. Other advantages of the use of autoclaves are the high rate and the degree of advancement of the reactions, the elimination of the loss of the volatile components, and the relative simplicity of standardizing the experiment conditions, which makes autoclaves very relevant to obtaining various materials based on the platinum group metals.

**Received:** July 14, 2011
**Revised:** August 9, 2011
**Published:** August 16, 2011

  

The production of bimetallic nanoparticles under the action of different types of physical effects is of great interest. For example, Takatani et al.[13] obtained binary Au/Pd and Au/Pt nanoparticles by the sonochemical reduction of aqueous solutions containing noble metal complexes and surfactants (sodium dodecyl sulfate or poly(ethylene glycol) monostearate). They found that the prepared nanoparticles exhibited different morphologies with the changing irradiation parameters and the surfactants.

To obtain noble metal nanoparticles, microwave irradiation is far more often used in comparison with ultrasound waves.[2,10,14,15] For example, Patel et al.[11] synthesized Pt, Pd, Pt−Ag, and Pd−Ag bimetal nanoparticles by the microwave polyol method and tried to understand the mechanism of the formation of mixed nanoparticles by attending to such experimental parameters as the in situ irradiation of mixed metal salts and the mixing of individual sols.

Microwave heating can provide the following advantages in comparison with the conventional heating: high heating rates, thus increasing the reaction rates; no direct contact between the heating source and the reactants and/or solvents; excellent control of the reaction parameters, which is important not only with respect to the quality of the product but also from the viewpoint of accident prevention; selective heating, if the reaction mixture contains compounds with different microwave-absorbing properties; higher yields; better selectivity due to the reduced side reactions; improved reproducibility; and automatization and high-throughput synthesis.[16] Microwave chemistry has some significant limitations. One of the major drawbacks is the high cost of dedicated microwave reactors. The short penetration depth of microwave radiation into a liquid medium limits the size of the reactors, which is a serious problem for scaling up. However, in spite of these limitations, microwave irradiation is widely applied at present for the intensification of various physicochemical processes both in the laboratory and in industry.[17]

With all of this going on, the processes of autoclave synthesis of finely dispersed particles of noble metals, especially under the action of microwave irradiation, have been insufficiently studied. There are, in fact, no data on the influence of external factors on the mechanisms of phase formation of finely dispersed particles of noble metals, on their compositions, or on their structures. The investigations of these processes are all important both for fundamental science and in practice.

The purpose of the present work is to study the reduction of gold(III) from muriatic solutions by nanocrystal palladium and platinum in autoclaves under the action of microwave irradiation.

## EXPERIMENTAL SECTION

Finely dispersed powders of palladium and platinum were synthesized according to refs 18 and 19. Muriatic acid was prepared by isothermal distillation in redistilled water. A solution of $HAuCl_4$ was prepared with the use of 1 M HCl.

The microwave oven was cycled as follows: on for 8 s and off for 12 s, with the total power always at 850 W. The temperature measurements were carried out with the use of a chromel-alumel thermocouple and a Testo 830-T2 IR thermometer.

All of the experiments were conducted in quartz autoclaves designed by us in accordance with the procedure published elsewhere[20] both under conventional heating conditions (air thermostat) and under the action of microwave irradiation (domestic microwave oven LG, with a 2.45 GHz working frequency).

Regardless of the heating method, this autoclave construction has a number of advantages: (i) the possibility of process observation; (ii) separation of the components of a reaction mixture prior to the beginning of the process; and (iii) autoclave rotation in a vertical plane that allows the realization of the maximum contact of phases. It is extremely important to the research of heterogeneous processes.

The quartz autoclave was filled with an aliquot of a muriatic solution of $HAuCl_4$. A portion of palladium black was placed in the fluoroplastic cup. For oxygen to be removed, the autoclave was positioned in an argon-filled chamber; the solution was bubbled with argon for 50 min and then was pressurized. Next, the autoclave was vertically inserted into the bore of the stock of an air thermostat that was preheated to a set temperature. After 30 min, the stirring was turned on. As a result, the solid and liquid phases were separately heated to the predetermined temperature and then brought into contact. As time passed, the autoclave was rapidly cooled. The precipitate was separated from the solution, repeatedly washed with distilled water to a negative test for chloride ions, and dried in vacuum at 60 °C to a constant weight.

X-ray diffraction (XRD) data were collected on a PANalytical X'Pert PRO MPD powder diffractometer. The analysis of the structure, microstructure, and quantitative phase composition of the materials was carried out using the Rietveld method.[21] XRD full-profile refinement was performed by derivative difference minimization.[22] The Au/Pd atomic ratio in the (Au, Pd) solid solution was estimated from the refined crystal lattice parameters assuming a linear relationship between the ratio and the parameter value. The XRD peak shape was approximated by the TCH pseudo-Voigt function,[23] taking into account the instrumental, microstrain, and crystal size contributions. An XRD pattern of a coarsely crystalline corundum sample was used for the instrumental broadening determination. The anisotropic broadening due to stacking faults was modeled according to ref 24.

The concentrations of metal ions in solution were found by atomic absorption (AAnalyst 400, PerkinElmer), inductively coupled plasma mass spectroscopy (Agilent-7500a), and spectrophotometric analysis. The amount of the solid phase was determined by gravimetric analysis.

The adsorption characteristics of the powders were obtained using a nitrogen adsorption method at 77 K (ASAP 2420, Micromeritics Inc.). Before being measured, the samples were heated to 70 °C and degassed at 1.2 Pa. The specific surface area was calculated from the adsorption isotherms according to the BET method.

The chemical composition of the solid phase was found by the dissolution of the powders accompanied by atomic absorption analysis with the use of an AAnalyst-400 spectrometer (PerkinElmer).

Transmission electron microscopy (TEM) analyses were performed using a JEOL JEM-2100 ($LaB_6$) equipped with an Oxford Inca x-sight energy dispersion spectrometer (EDS); the accelerating voltage was 200 kV. Scanning electron microscopy (SEM) analyses were performed using a Hitachi S5500 microscope equipped with a Thermo Scientific Noran Spectral System EDS.

The X-ray photoelectron spectra were acquired using a SPECS photoelectron spectrometer equipped with a Mg K$\alpha$ X-ray source (1253.6 eV) and a PHOIBOS 150 MCD-9 analyzer at an analyzer pass energy of 8 eV (narrow scans) and an electron takeoff angle of 90°.

## RESULTS AND DISCUSSION

**Au−Pd.** The specific surface area of the initial palladium black, determined by the adsorption analysis, was 36 $m^2/g$. Figure 1 shows that the particles are nearly spherical in shape and aggregate with each other in long chains. According to the full-profile analysis of the XRD pattern (Figure 1), the crystallite sizes amount to 10 nm. These data correspond to the specific surface area value.

Previously, it had been found[25] that palladium black in muriatic acid solutions of palladium(II) chloride was coarsened with the rate of growth, depending on the temperature. Thus,

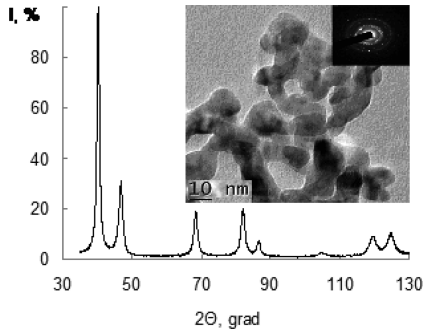


**Figure 1.** XRD pattern and TEM image of the initial Pd.

after 60 min of reaction at 130 °C, the average particle size increased from 40 to 65 nm whereas at 180 °C it totaled 150−200 nm. In the absence of palladium ions in the solution, no structural changes in Pd(0) were found. This fact allowed us to assume an electrochemical mechanism of coarsening. In the case of the contact of two or more of palladium blocks with different dimensions and consequently different potentials, a chain consisting of concatenated short-circuit galvanic cells arises. As a result, smaller blocks dissolve and larger ones increase:

$$Pd^0(r_1) = Pd^{2+} + 2e$$
$$Pd^{2+} + 2e = Pd^0(r_2)$$

During the interaction of finely dispersed palladium with muriatic solutions, the partial dissolution of palladium takes place according to reaction 1:

$$2Pd^0 + O_2 + 8HCl \rightarrow 2H_2PdCl_4 + 2H_2O \quad (1)$$

Previously,[25] this process was proven to proceed in an inert atmosphere because of oxygen chemisorbed at the palladium surface and to be completed in 15 min at 130 °C.

The solubility of the 10 nm palladium powder particles in 1 M muriatic solution amounts to 5% from the initial weight of the palladium powder. These data are consistent with the specific surface area value.

The interaction of palladium with muriatic solutions of $HAuCl_4$ proceeds according to reaction 2:

$$2HAuCl_4 + 3Pd^0 + 4HCl \rightarrow 2Au^0 + 3H_2PdCl_4 \quad (2)$$

The thermodynamic estimate shows that the Gibbs energy of this reaction is −235 kJ (at 25 °C). The equilibrium of this reaction is heavily displaced in the direction of the products ($K = 1.6 \times 10^{41}$). The molar ratio of $n_{Pd}/n_{Au}$ equals 4.

The process of the interaction of Pd(0) and Au(III) is likely to include the Au(I) formation stage. In acidic media, Au(I) is unstable and disproportionates according to reaction 3:[26]

$$Au^+ \rightarrow Au^0 + Au^{3+} \quad (3)$$

This process proceeds quickly enough that Au(I) is not registered in the solution. Thus, Au(0) accumulates in the solid phase.

An investigation of the process of the contact reduction of Au(III) by palladium was conducted at 110 and 130 °C, and thereafter the conventional and microwave techniques of heating were compared.

In the given temperature range, the interaction between palladium black and muriatic solutions of gold begins as soon as they are brought into contact with one another. About 1 min later, the solution begins to change color from yellow to red-brown. It should be noted that in the case of microwave heating there were no visual changes in the system after 10−15 min from the beginning of the experiment whereas in the case of conventional heating the color of the solution became invariable after 20 min.

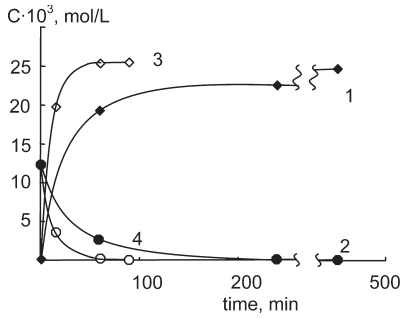


**Figure 2.** Kinetic curves of Pd(II) (1, 3) and Au(III) (2, 4) concentrations in the solution. Open markers denote microwave heating; solid markers denote thermal heating at 110 °C.

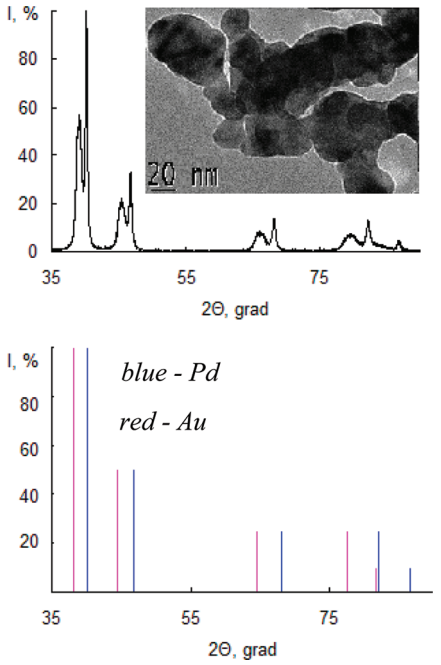


**Figure 3.** XRD pattern and TEM image of bimetallic Au/Pd after 60 min of thermal heating.

Figure 2 shows the kinetic curves of the change in concentration of gold and palladium ions in the solutions. As can be seen from the figure, gold(III) was completely reduced in the solutions in all experiments at 110 °C. In the case of microwave heating in comparison with conventional heating, the time when the concentration of palladium in the solutions did not vary was reduced by a factor of 4.

Figure 3 shows XRD pattern and the TEM image of the samples. According to the transmission electron micrograph of the Au/Pd formed particles, in the case of thermal heating the particles were coarsened after an hour of contact reduction, thus the length of the chains was essentially decreased.


dx.doi.org/10.1021/la202686x |*Langmuir* 2011, 27, 11697–11703

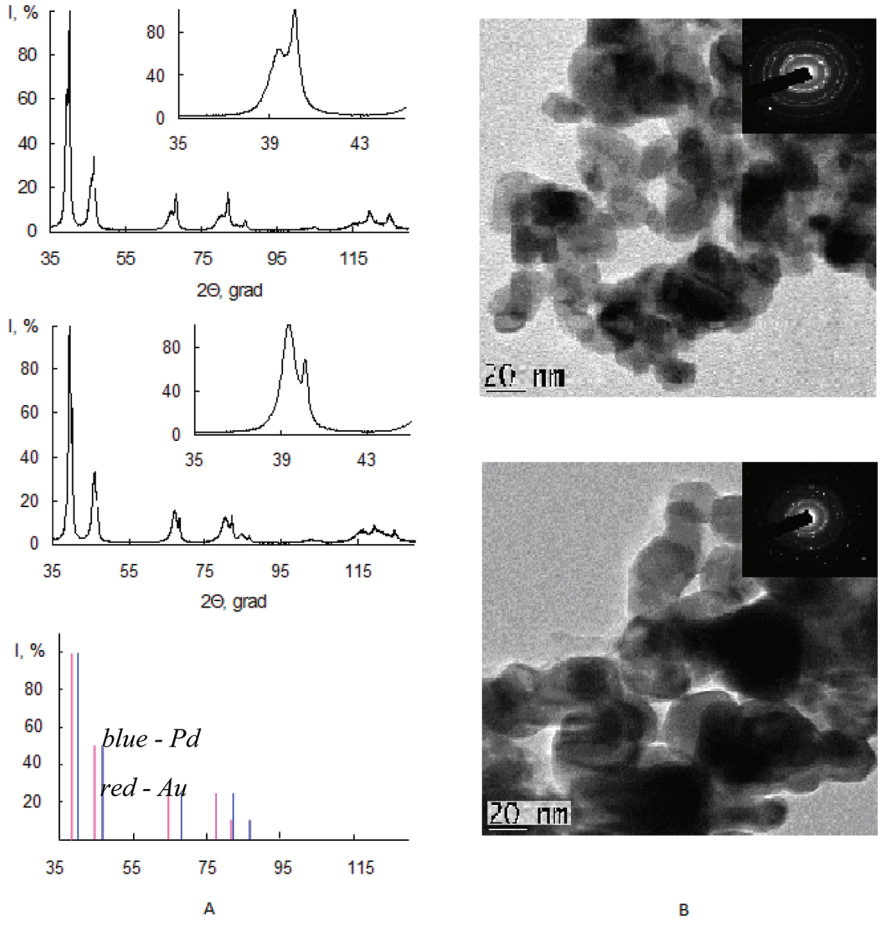


**Figure 4.** (A) XRD pattern and (B) TEM images of bimetallic Au/Pd: top, after 15 min of microwave heating; bottom, after 60 min of microwave heating.

The X-ray analysis showed that in all cases the obtained solid particles consisted of two phases: finely dispersed palladium and a substitutional (Au, Pd) solid solution. The formation of the latter one can be explained by the simultaneous precipitation of palladium due to the electrochemical recrystallization process (as shown above) and gold owing to its chemical reduction (reactions 2 and 3).

As quickly as 30 min after the reaction began under the conditions of conventional heating, the solid phase contained 39% of the solid solution with a Au/Pd ratio of 53/47. After 1 h, the content of the solid solution increased up to 50% and the Au/Pd ratio in the solution became 60/40. In the case of microwave heating, only 15% of Pd(0) remained in the powder under the conditions of the same time of reaction and a similar quantitative composition of the solid solution. Figure 4 shows fragments of XRD patterns (A) and the SEM images (B) of the samples obtained under microwave heating. It should be pointed out that when the time of the experiments is increased by more than 60 min, the XRD pattern form remains practically constant.

We established in previous work[27] that the increasing temperature of up to 130 °C did not result in the complete reduction of Au(III) from the solution in spite of surplus palladium in the solid phase. It is presumably connected with the isolation of palladium from the solution.

Metallic palladium is known to transform into a water-soluble form ($Pd^{2+}$) in nitric acid solutions. Confirming the hypothesis about palladium isolation, the obtained samples were treated for a long time with a hot solution of nitric acid. At the same time, there was no dissolution of palladium.

The reason is probably that the melting point, in particular, of gold can decrease considerably as the particles decrease in size. And during the transition from the bulk state to the finely dispersed state, the decreasing temperature takes on an exponential character.[28] As a result, on the one hand, the diffusion of gold atoms along the grain boundaries of palladium particles takes place, which is one of the reasons for the formation of the substitutional (Au,Pd) solid solution, and on the other hand, an effect of gold "submelting" is observed. The latter results in the formation of a shell of Au(0) on the surface of the solid-phase particles and their isolation from the solution.

According to the X-ray diffraction and nitrogen adsorption methods, after 4 h of the contact reduction of Au(III) by palladium with 40 nm crystallites, the average size of the obtained bimetallic particles was 100 nm. Figure 5 shows X-ray photoelectron spectra of the bimetallic Au/Pd products before and after $Ar^+$ etching. The Pd $3d_{5/2,3/2}$ doublet is overlapped by a stronger Au $5d_{5/2}$ band; the convolution of the spectra allows us to find atomic Au/Pd ratios of 18, 13, and 7 before and after $Ar^+$ sputtering ($Ar^+$ ion energy of 5 kV with an ion current of 30 $\mu$A) for 2 and 10 min, respectively. The binding energies of Au $4f_{7/2}$ (84.0 eV) and Pd $3d_{5/2}$ (335.1 eV) correspond to elemental metals. The atomic Au/Pd ratio at the surface equal to 18:1


dx.doi.org/10.1021/la202686x |*Langmuir* 2011, 27, 11697–11703

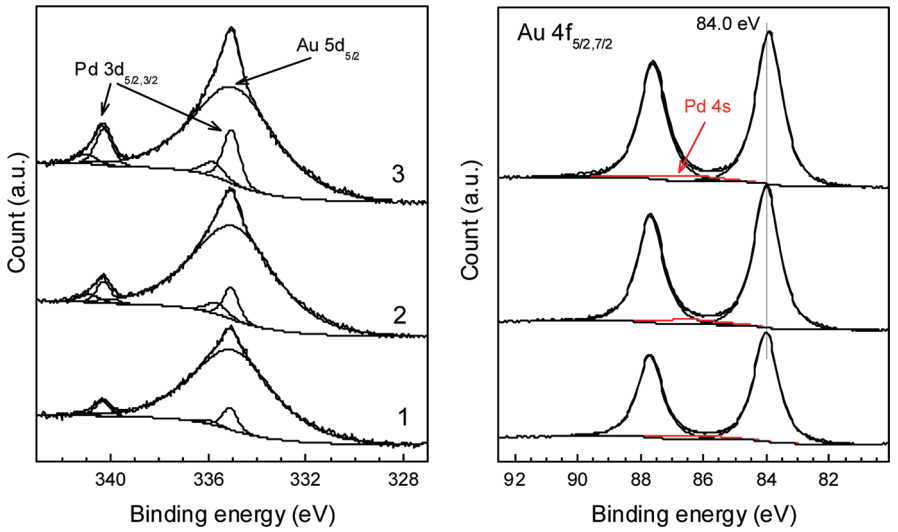


**Figure 5.** X-ray photoelectron spectra of Pd−Au nanoparticles acquired (1) before and after $Ar^+$ sputtering for (2) 2 and (3) 10 min ($Ar^+$ energy of 5 kV with an ion current of 30 $\mu$A).

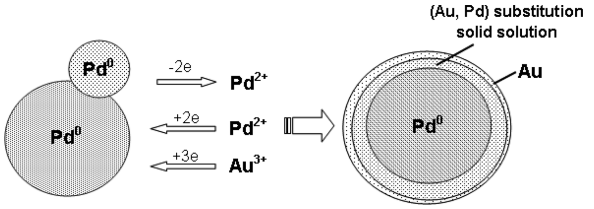


**Figure 6.** Core−shell Au/Pd particle formation scheme.

corresponds to 95 atom % gold. This value reflects the composition of several surface atomic layers. The layer directly adjoining the solution should be even more enriched by gold. The palladium content increases from the particle surface to its center. Further etching shows more and more increasing content of palladium. These facts indicate that gold forms a shell above the Pd or Pd−Au core.

Thus, the formed Au−Pd particles have the core-shell structure with the palladium core surrounded by the substitutional (Au, Pd) solid solution. This is confirmed by the X-ray data. Figure 6 shows the core−shell Au/Pd particle formation scheme.

The XRD patterns of the solid phase obtained by conventional heating differ from those obtained by the action of microwave irradiation. In the case of conventional heating, the peaks are asymmetric and strongly widened. In our opinion, this is connected with the inhomogeneity of the solid solution composition. It is gold-deficient near the palladium core and enriched by gold at the periphery of the particle. In the case of microwave heating, the peaks are more symmetric and less widened. This fact points to the higher chemical homogeneity of the solid solution, which can be explained by the presence of a skin effect originating from the action of microwave irradiation. Owing to this, the local overheating of the solid phase and increasing rates of atom diffusion along the grain boundaries are observed.

Thus, we assume that there are two mechanisms of formation of the substitutional (Au, Pd) solid solution: the first one is due to the simultaneous precipitation of palladium and gold atoms, and the second one is related to atom diffusion along the grain boundaries.

**Au−Pt.** The initial platinum powders were investigated by the nitrogen adsorption method; the results are presented in Table 1.

**Table 1. Specific Surface Area of the Initial Platinum Powders**

| sample of Pt powder | no. 1 | no. 2 |
|---|---|---|
| S, $m^2/g$ | 1.1 | 10 |

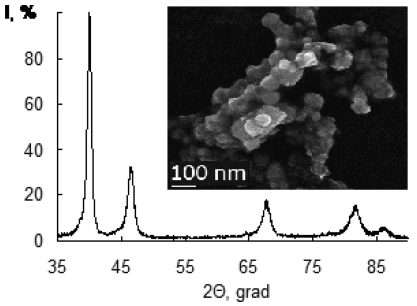


**Figure 7.** XRD pattern and SEM image of initial Pt.

Figure 7 shows the XRD pattern of Pt(0) powder with a specific surface area of 10 $m^2/g$. According to the X-ray analysis, the platinum particle size amounts to 30 nm, correlating satisfactorily with the specific surface area value and the electron microscopy data (Figure 7). Unlike palladium black, platinum demonstrates just a slight coarsening at 130 °C.

In terms of thermodynamics, gold can be reduced by both Pt(0) and Pt(II):

$$2[AuCl_4]^- + 3Pt + 4Cl^- = 2Au + 3[PtCl_4]^{2-} \quad (4)$$

$$2[AuCl_4]^- + 3[PtCl_4]^{2-} = 2Au + 3[PtCl_6]^{2-} + 2Cl^- \quad (5)$$

$\Delta G = -160$ kJ for reaction 4, and $\Delta G = -185$ kJ for reaction 5 at 25 °C.

In our experiments, the molar ratio of $n_{Pt}/n_{Au}$ was equal to 2.

At 130 °C, platinum(II) quantitatively reduces gold(III) from the solution. Reaction 5 is completed quickly enough, in 10−15 min, and within an hour, gold coarsens to quite large particles.


dx.doi.org/10.1021/la202686x |*Langmuir* 2011, 27, 11697–11703

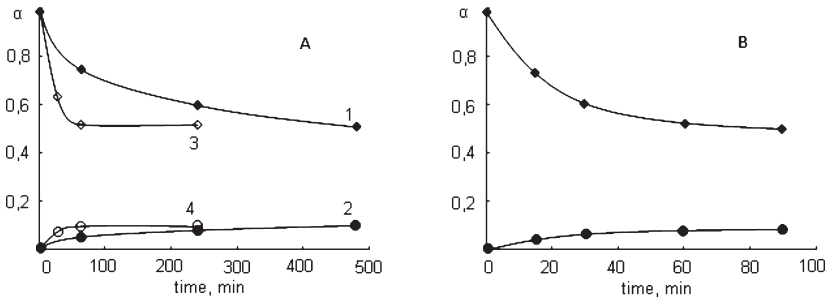


**Figure 8.** (A) Degree of Au(III) consumption (1, 3) and Pt(IV) (2, 4) accumulation in the solution. Solid symbols denote initial platinum black no. 1, and open markers denote initial platinum black no. 2 (Table 1). $T$ = 130 °C. Thermal heating. (B) Degree of Au(III) consumption (♦) and Pt(IV) accumulation (●) in the solution. $T$ = 110 °C. Microwave heating.

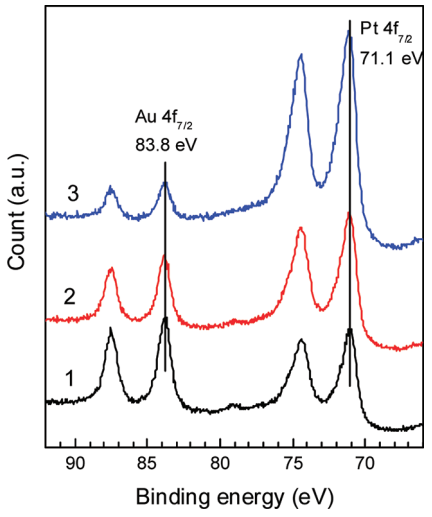


**Figure 9.** X-ray photoelectron Au 4f and Pt 4f spectra of Pt−Au nanoparticles acquired (1) before and after $Ar^+$ sputtering for (2) 2 and (3) 10 min ($Ar^+$ ion energy of 5 kV with an ion current of 30 $\mu$A). The obtained value is in good agreement with the electron microscopy (Figure 10), nitrogen adsorption, and chemical analysis data.

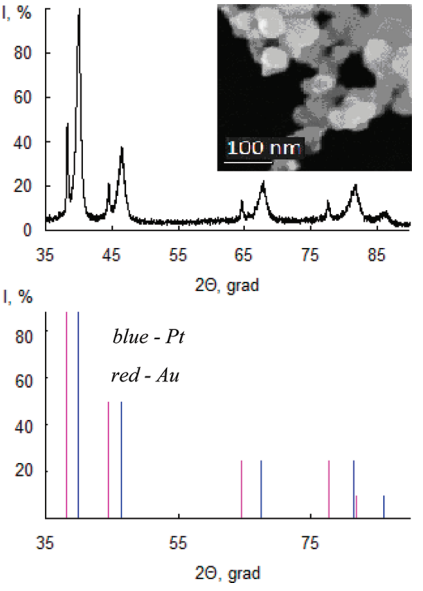


**Figure 10.** XRD pattern and SEM image of bimetallic Au/Pt (thermal heating at 130 °C).

The changes in the concentrations of the platinum and gold ions in the solution are determined by reaction 6:

$$4[AuCl_4]^- + 3Pt + 2Cl^- = 4Au + 3[PtCl_6]^{2-} \qquad (6)$$

The equilibrium of this reaction is heavily displaced in the direction of the products ($K = 1.1 \times 10^{66}$). The investigation of the process was conducted in the temperature range from 90 to 130 °C, and thereafter the conventional and microwave techniques of heating were compared.

With platinum black no. 2, at 130 °C the cementation process starts quickly enough. In the case of conventional heating, according to the atomic absorption data, about 40% of the gold was reduced from the solution in 30 min, and in an hour, the degree of reduction was about 50% (Figure 8A). XPS shows the presence both of Au and Pt at the particle surfaces, with their contents being 39 and 61 atom %, respectively (Figure 9, curve 1). The intensity of the Au line (83.8 eV) decreases, and that of the Pt line (71.1 eV) grows (Figure 9) because of $Ar^+$ etching, so the Pt/Au ratio increases from 2.2 to 10, indicating that the content of gold is the highest at the surface and rapidly decreases toward the particle core.

Further increases in the time did not result in a higher degree of advancement of the reaction; some of gold(III) remained in the solution in spite of surplus Pt(0). A possible explanation of this fact is the effect of gold "submelting", as in the case of the Au−Pd system, and the formation of the gold shell on the surfaces of the platinum particles. For microwave heating, about 50% of the gold was reduced from the solution even at 110 °C with a significant decrease in the experimental time (Figure 8B).

The time of the contact reduction process was considerably increased when platinum black no. 1 was used.

Although this process is thermodynamically allowable, it is so hindered kinetically in the case of conventional heating at 90 °C that platinum powder no. 1 did not reduce gold from the solution for 4 h. The chemical analysis did not reveal Au(0) in the solid phase. Using microwave irradiation allowed the removal of kinetic limitations: according to the atomic absorption analysis, about 20% of the gold was reduced from the solution in 90 min.

At 130 °C, the degree of the reduction of gold was no more than 50%, as for platinum powder no. 2, but the constancy of the concentrations of platinum and gold ions in the solution was not reached for a long period of time.

The XRD data (Figure 10) showed that in all cases the precipitates contained two phases, platinum and gold, in contrast

with the Au−Pd system, in which the solid solution was not registered.

The obtained results allow us to propose that the process of the interaction of finely dispersed platinum with muriatic solutions of gold(III) is limited by reaction 4. The rate of reaction 5 is much higher and Pt(II) is not registered in the solution. As a consequence, gold deposits not only on the surface of platinum but also in the form of separate particles that coarsen into quite large particles.

## CONCLUSIONS

The interaction of finely dispersed palladium powder with muriatic solutions of gold was found to result in the production of particles consisting of the palladium core surrounded by the substitutional (Au, Pd) solid solution. The formation of the latter one can be explained, on one hand, by the simultaneous precipitation of palladium due to the electrochemical recrystallization process and gold owing to its chemical reduction, and, on the other hand, by the diffusion of atoms along the grain boundaries. In contrast to the Au−Pd system, the solid solution in the Au−Pt one was not obtained; the particles consisted of a platinum core surrounded by a gold layer, in spite of the fact that in both cases the phase diagrams are characterized by an unlimited line of solid solutions. One can say with a fair degree of confidence that the decisive role in the formation of solid solutions belongs to the ratio between the aggregation and reduction rates. If they are comparable, then a solid solution is formed; otherwise, a mechanical mix is produced. Using microwave irradiation not only accelerates the synthesis process of particles but also allows us to obtain more homogeneous materials in comparison to conventional heating, as has been demonstrated with the example of the Au−Pd system.

## AUTHOR INFORMATION

### Corresponding Author

*E-mail: ov_bel@icct.ru.

## REFERENCES

(1) Ershov, B. G. *Mendeleev Chem. J.* **2001**, *XLV*, 20–30.
(2) Harpeness, R.; Gedanken, A. *Langmuir* **2004**, *20*, 3431–3434.
(3) Thompson, D. *Platinum Met. Rev.* **2004**, *48*, 169–172.
(4) Thompson, D. *Nano Today* **2007**, *2*, 40–43.
(5) Villa, A.; Campione, C.; Prati, L. *Catal. Lett.* **2007**, *115*, 133.
(6) Devarajan, S.; Bera, P.; Sampath, S. *J. Colloid Interface Sci.* **2005**, *290*, 117–129.
(7) Wu, M.-L.; Chen, D.-H.; Huang, T.-Ch *J. Am. Chem. Soc.* **2001**, *56*, 127–134.
(8) Mandal, S.; Mandale, A. B.; Sastry, M. *J. Mater. Chem.* **2004**, *14*, 2868–2871.
(9) Guo, Sh.; Wang, L.; Dong, Sh.; Wang, E. *J. Phys. Chem C* **2008**, *112*, 13510–13515.
(10) Tsuji, M.; Hashimoto, M.; Nishizawa, Y.; Kubokawa, M. *Chem.−Eur. J.* **2005**, *11*, 440–452.
(11) Patel, K.; Kapoor, S.; Dave, D. P.; Mukherjee, T. *J. Chem. Sci.* **2005**, *117*, 311–316.
(12) Torres-Castro, A.; Ferrer, D.; Sepulveda-Guzman, S.; Mendez, U. O. *Microsc. Microanal.* **2007**, *13*, 568–569.
(13) Takatani, H.; Kago, H.; Nakanishi, M.; Kobayashi, Y. *Rev. Adv. Mater. Sci.* **2003**, *5*, 232–238.
(14) Mallikarjuna, N. N.; Varma, R. S. *Cryst. Growth Design* **2007**, *7*, 686–690.
(15) Horikoshi, S.; Abe, H.; Torigoe, K.; Abe, M.; Serpone, N. *Nanoscale* **2010**, *2*, 1441–1447.
(16) Bilecka, I.; Niederberger, M. *Nanoscale* **2010**, *2*, 1358–1374.
(17) Shi, S.; Hwang, J.-Y. *J. Miner. Mater. Charact. Eng.* **2003**, *2*, 101–110.
(18) Kovalenko, N. L.; Belousov, O. V.; Dorokhova, L. I.; Zharkov, S. M. *Russ. J. Inorg. Chem.* **1995**, *40*, 678.
(19) Belousov, O. V.; Kovalenko, N. L.; Dorokhova, L. I.; Chumakov, V. G. *Russ. J. Inorg. Chem.* **2001**, *46*, 603–607.
(20) Kovalenko, N. L.; Dorokhova, L. I. *Russ. J. Inorg. Chem.* **1991**, *36*, 2571.
(21) Rietveld, H. M. *J. Appl. Crystallogr.* **1969**, *2*, 65–71.
(22) Solovyov, L. A. *J. Appl. Crystallogr.* **2004**, *37*, 743–749.
(23) Thompson, P.; Cox, D. E.; Hastings, J. B. *J. Appl. Crystallogr.* **1987**, *20*, 79–83.
(24) Solovyov, L. A. *J. Appl. Crystallogr.* **2000**, *33*, 338–343.
(25) Belousov, O. V.; Dorokhova, L. I.; Solov'ev, L. A.; Zharkov, S. M. *Russ. J. Phys. Chem.* **2007**, *81*, 1303.
(26) Mironov, I. V.; Tsvelodub, L. D. *Russ. J. Inorg. Chem.* **2000**, *45*, 706.
(27) Belousov, O. V.; Belousova, N. V.; Burlo, A. V. *Smart Nanocompos.* **2010**, *1*, 91–97.
(28) Buffat, Ph.; Borel, J.-P. *Phys. Rev. A* **1976**, *13*, 2287.